Lab on a Chip

Micro- & nano- fluidic research for chemistry, physics, biology, & bioengineering

www.rsc.org/loc

Volume 11 | Number 13 | 7 July 2011 | Pages 2121–2296

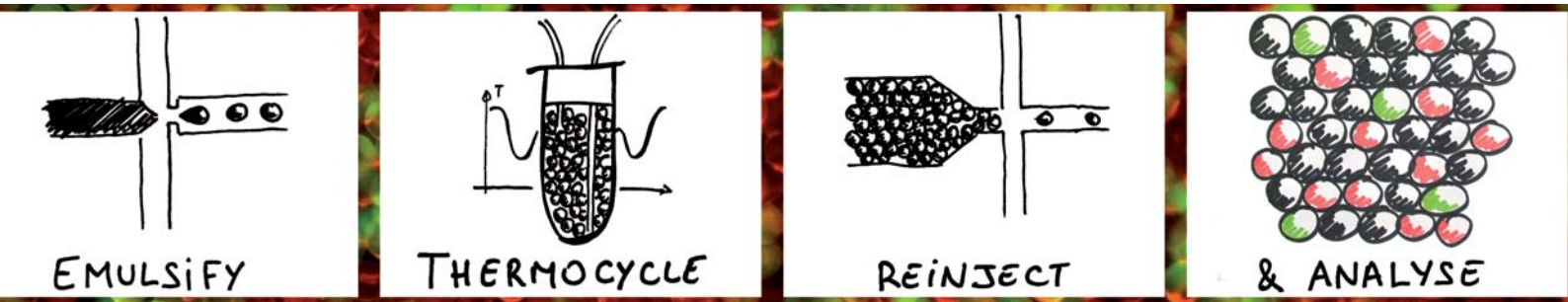

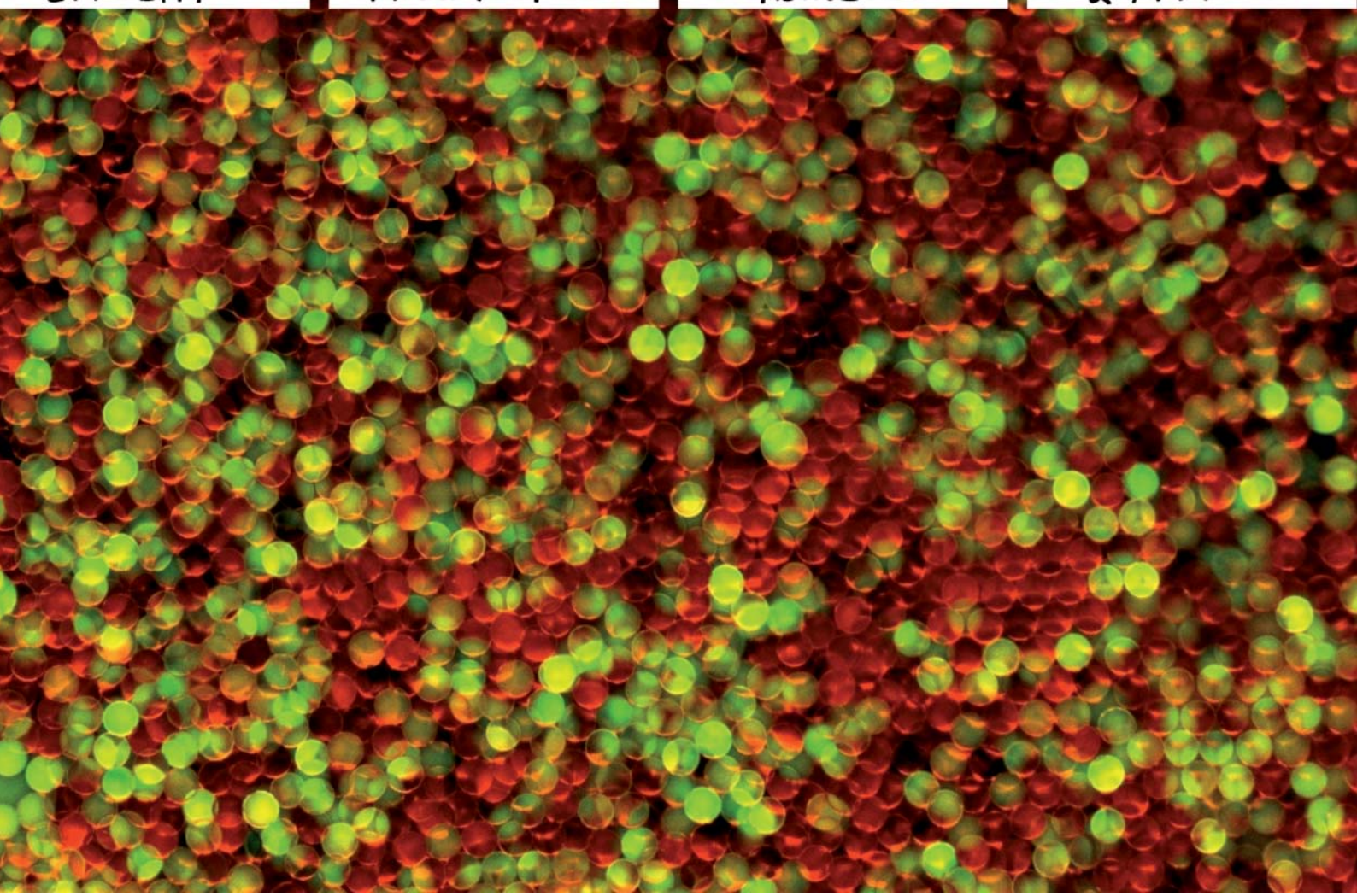

ISSN 1473-0197

RSC Publishing

PAPER

Valérie Taly *et al.*

Quantitative and sensitive detection of rare mutations using droplet-based microfluidics

Lab on a Chip

Dynamic Article Links

Cite this: *Lab Chip*, 2011, **11**, 2156

www.rsc.org/loc

PAPER

Quantitative and sensitive detection of rare mutations using droplet-based microfluidics†

Deniz Pekin,[a] Yousr Skhiri,[a] Jean-Christophe Baret,[ac] Delphine Le Corre,[b] Linas Mazutis,[a] Chaouki Ben Salem,[a] Florian Millot,[a] Abdeslam El Harrak,[d] J. Brian Hutchison,[e] Jonathan W. Larson,[e] Darren R. Link,[e] Pierre Laurent-Puig,[b] Andrew D. Griffiths*[a] and Valérie Taly*[a]

Received 14th February 2011, Accepted 4th April 2011
DOI: 10.1039/c1lc20128j

Somatic mutations within tumoral DNA can be used as highly specific biomarkers to distinguish cancer cells from their normal counterparts. These DNA biomarkers are potentially useful for the diagnosis, prognosis, treatment and follow-up of patients. In order to have the required sensitivity and specificity to detect rare tumoral DNA in stool, blood, lymph and other patient samples, a simple, sensitive and quantitative procedure to measure the ratio of mutant to wild-type genes is required. However, techniques such as dual probe TaqMan® assays and pyrosequencing, while quantitative, cannot detect less than ~1% mutant genes in a background of non-mutated DNA from normal cells. Here we describe a procedure allowing the highly sensitive detection of mutated DNA in a quantitative manner within complex mixtures of DNA. The method is based on using a droplet-based microfluidic system to perform digital PCR in millions of picolitre droplets. Genomic DNA (gDNA) is compartmentalized in droplets at a concentration of less than one genome equivalent per droplet together with two TaqMan® probes, one specific for the mutant and the other for the wild-type DNA, which generate green and red fluorescent signals, respectively. After thermocycling, the ratio of mutant to wild-type genes is determined by counting the ratio of green to red droplets. We demonstrate the accurate and sensitive quantification of mutated *KRAS* oncogene in gDNA. The technique enabled the determination of mutant allelic specific imbalance (MASI) in several cancer cell-lines and the precise quantification of a mutated *KRAS* gene in the presence of a 200 000-fold excess of unmutated *KRAS* genes. The sensitivity is only limited by the number of droplets analyzed. Furthermore, by one-to-one fusion of drops containing gDNA with any one of seven different types of droplets, each containing a TaqMan® probe specific for a different *KRAS* mutation, or wild-type *KRAS*, and an optical code, it was possible to screen the six common mutations in *KRAS* codon 12 in parallel in a single experiment.

Introduction

A complex array of genetic alterations exists in most human cancer cells: deletions, amplifications, point mutations and chromosomal rearrangements all play a major role in the development and progression of cancers.[1,2] Somatic mutations can, therefore, serve as biomarkers that allow tumor cells to be distinguished from their normal counterparts.[3] Mutations within tumor cells and in DNA released by tumor cells into clinical samples, such as blood, lymph, stools or urine, can be used to detect cancers.[4,5] Furthermore, tumor-specific genetic changes can have a profound impact on clinical decision-making and outcome.[6]

In order to use tumor-specific somatic mutations as biomarkers for clinical oncology, the mutations must be detected in a large excess of non-mutated DNA from normal cells. The majority of genetic tests are based on the polymerase chain reaction (PCR), which is the most sensitive method for the detection of rare species in a complex sample. Highly sensitive methods have been developed to preferentially enrich mutant sequences present at low concentrations in a background of wild-type DNA in clinical samples and selectivity of up to 10^{-9} has been described (see ref. 7 for a review). However, such assays are

[a]*Institut de Science et d'Ingénierie Supramoléculaires (ISIS), Université de Strasbourg, CNRS UMR 7006, 8 allée Gaspard Monge, BP 70028, F-67083 Strasbourg Cedex, France. E-mail: griffiths@unistra.fr; vtaly@unistra.fr*
[b]*Université Paris Descartes, INSERM UMR-S775, Centre Universitaire des Saints-Pères, 45 rue des Saints-Pères, 75270 Paris Cedex 06, France*
[c]*Max-Planck-Institute for Dynamics and Self-organization, Am Fassberg 17, D-37077 Göttingen, Germany*
[d]*RainDance Technologies France, 8 allée Gaspard Monge, BP 70028, F-67083 Strasbourg Cedex, France*
[e]*RainDance Technologies, Lexington, MA 02421, Massachusetts, USA*
† Electronic supplementary information (ESI) available: Statistical analysis and confidence intervals for the dilutions, tables and figures. See DOI: 10.1039/c1lc20128j

qualitative, which has two disadvantages. First, an assay can yield a false-negative result (inadequate sensitivity) because the amount of starting DNA is too low to detect rare mutations. Second, an assay can yield a stochastic false-positive result (inadequate specificity) because, for example, rare random mutations are present in a sample.

Quantitative technologies, however, can overcome these problems. They have the ability to directly measure the number of DNA molecules tested per assay and therefore ensure that the amount of starting material is sufficient to detect rare mutations in the predicted frequency range. Quantification also allows random and pathogenic mutations to be distinguished by establishing a baseline mutant-to-wild-type ratio (the background mutation frequency of human cells). Quantitative assays also allow standard quality control monitoring which is a necessary requirement for routine diagnostic testing.[8] Most quantitative assays are analog in nature: an average signal is acquired from the mutant and wild-type DNA molecules present in the sample and the ratio between the mutant and wild-type signal is an estimate of the mutation frequency.[3,9–11] However, commonly used analog assays have limited sensitivity. Frequently used techniques like pyrosequencing[12–14] or real-time PCR[15,16] have sensitivities ranging from 1% to 10% for the detection of mutant gDNA diluted in wild-type gDNA (see ref. 17 for a review).

More precise and sensitive quantification of mutated DNA is possible using digital techniques, which allows the analysis of many individual DNA molecules.[3] One of the most important techniques is digital PCR, which is based on the compartmentalization and amplification of single DNA molecules.[18,19] Digital PCR allows the discrete counting of the mutant and wild-type alleles present in a sample. Its sensitivity is only limited by the number of molecules that can be analyzed and the false positive rate of the mutation detection assay. Digital assays are particularly well suited for the analysis of clinical samples like stool or plasma where tumor derived DNA fragments represent only a small fraction of the total DNA[20] and digital PCR has been used for detection of *KRAS* mutations in various clinical samples.[19,21–23]

The original microtitre plate-based digital PCR techniques were, however, both slow and expensive. To address these issues, several miniaturized methods allowing millions of single-molecule PCR reactions to be performed in a single assay have been developed.[3] Single-molecule PCR in a polyacrylamide film can be used to generate discrete DNA colonies (polonies).[24] Alternatively, single-molecule PCR reactions can be performed on beads in picotiter plates,[25] or in aqueous droplets in water-in-oil emulsions (BEAMing).[26,27] After recovering the beads, hybridization of fluorescently labeled oligonucleotides[26] or single base extension (SBE) with fluorescently labeled dideoxynucleotides[28] is used for sequence differentiation and the beads are analyzed by flow cytometry. The resulting highly sensitive digital procedure has found many applications including single-molecule reverse-transcription PCR,[29] or detection and enumeration of rare genetic mutations.[26] For example, BEAMing followed by SBE and flow cytometry was used to quantify the level of mutated DNA circulating in the plasma of colorectal cancer patients.[30] The detection limit, determined by the error rate of the DNA polymerase used for the pre-amplification of the plasma DNA, was one mutant DNA molecule in a background of 10 000 wild-type DNA molecules.

Other strategies for digital PCR are based on microfluidic technology. Digital PCR has been performed by spatial separation of PCR reactions in capillary systems.[31] Digital PCR in nanolitre microcompartments defined by pneumatic valves[32,33] has been applied to various applications including single-cell gene expression analysis,[34] copy-number evaluation[35] and single nucleotide polymorphism genotyping.[36,37] However, none of these procedures can analyze more than several thousand reactions in parallel.

An alternative strategy is to perform digital PCR in aqueous droplets separated by oil in microfluidic systems.[38–41] In contrast to classical procedures used to create emulsions, droplet-based microfluidic systems allow the creation of highly monodisperse droplets (<1.5% polydispersity) and precise manipulation of the droplets.[42] Droplets of microlitre to nanolitre volume also allow several thousands of PCR reactions to be performed in parallel.[43–45] However, a further reduction in assay volume and increase in processivity is necessary to perform highly sensitive assays, which require millions of parallel PCR reactions. To analyze millions of reactions, digital PCR can be performed using picolitre droplets, which can be generated and manipulated at kHz frequencies in microfluidic systems. Real-time PCR amplification using fluorescent probes to monitor DNA amplification has been performed directly in picoliter droplets in microfluidic systems,[38,39,41,46] as has reverse-transcription real-time PCR (RT-rtPCR),[47] isothermal amplification of single DNA molecules[48] and DNA amplification using primer functionalized microbeads.[49]

In this manuscript, we describe the development and validation of a method, based on digital PCR, which allowed the highly sensitive and quantitative detection of mutations in the *KRAS* oncogene[50,51] within a large excess of wild-type sequences (Fig. 1). Using a microfluidic system, single target DNA molecules were compartmentalized in microdroplets together with clinically validated fluorogenic TaqMan® probes specific for mutated and wild-type *KRAS*,[15] thermocycled and the fluorescence of each droplet measured. The amplification of mutant DNA gave a green-fluorescent droplet while the amplification of wild-type DNA gave a red-fluorescent droplet and the ratio of mutant to wild-type DNA was determined from the ratio of green to red droplets. This strategy is both highly quantitative and highly sensitive. It enabled the precise determination of mutant allelic specific imbalance (MASI) in several cancer cell-lines and the precise quantification of a single mutated *KRAS* gene in a background of 200 000 unmutated *KRAS* genes. Furthermore, it was possible to screen the six common mutations in *KRAS* codon 12 in parallel in a single experiment.

Results

Quantification of mutated and wild-type *KRAS* DNA: determination of the mutant allelic fraction in different cell-lines

We developed a microfluidic procedure, based on digital PCR in picoliter volume droplets, to measure the ratio of mutant and wild-type genes in gDNA extracted from cell-lines. The basic procedure involves 3 major steps (Fig. 1): (i) emulsification of PCR reagents, primers and TaqMan® probes specific for mutant and wild-type DNA together with gDNA at a concentration equivalent to less

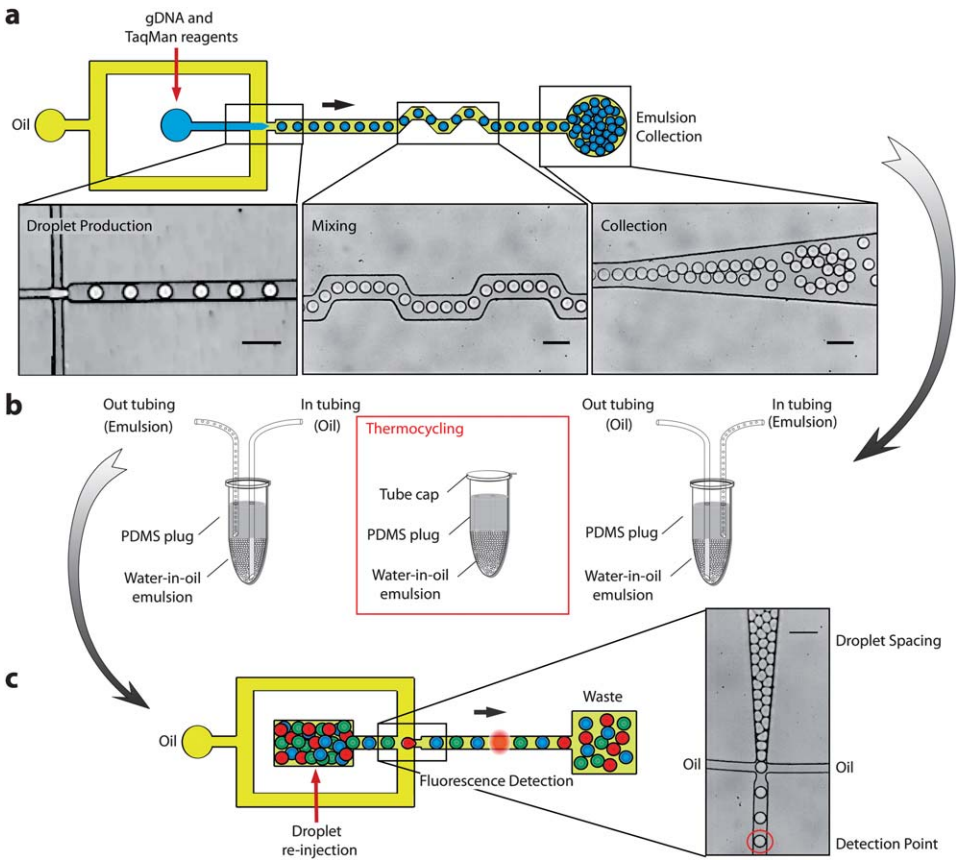

Fig. 1 Overview of the system. (a) An aqueous phase containing the gDNA, PCR reagents and TaqMan® probes specific for the wild-type and mutant genes is emulsified within a microfluidic device. Light micrographs of drop production, mixing, and collection are shown (scale bars 60 μm). The concentration of gDNA is such that there is, on average, less than one (haploid) genome equivalent per droplet. (b) The emulsion is collected in a PDMS-sealed tube (the collection/reinjection device) and thermocycled. During DNA amplification, the TaqMan® probes are cleaved and the corresponding fluorophores are released. TaqMan® probes specific for the mutant sequence carry a 6-FAM fluorophore (λ_{ex} 494 nm/λ_{em} 522 nm) and TaqMan® probes specific for the wild-type sequence carry a NED fluorophore (λ_{ex} 546 nm/λ_{em} 575 nm). Thus the amplification of mutant DNA gives green-fluorescent droplets while the amplification of wild-type DNA gives red-fluorescent droplets. (c) The emulsion is then reinjected onto a microfluidic chip, the droplets are spaced by oil, and the fluorescent signal of each droplet is analyzed. A light micrograph of re-injection and spacing is shown (scale bar 60 μm).

than one (haploid) genome equivalent per droplet; (ii) thermocycling of the emulsion to perform the PCR reaction; and (iii) measurement of the fluorescence of each droplet.

Mutations in *KRAS* are amongst the most common oncogenic alterations in a range of human cancers. The *KRAS* oncogene is constitutively activated by a small set of specific mutations which almost all occur in codons 12 and 13 of exon 2.[50] We used the system to quantify mutations in codons 12 and 13 of the *KRAS* oncogene in gDNA extracted from six different human cell-lines (see Experimental): (i) a homozygous cell-line bearing a wild-type *KRAS* gene (SW48); (ii) a homozygous cell-line bearing a mutated *KRAS* gene (SW620); and (iii) four different heterozygous cell-lines (H1573, H358, LoVo and LS123) bearing wild-type and mutated *KRAS* genes with a different mutation in each cell-line (Table 1). 6 μg of gDNA from each cell-line was compartmentalized in 9 pL droplets (for H358, LoVo, SW620 and SW48 cell-lines) or 4 pL droplets (for LS123 and H1573 cell-lines) together with PCR reagents, primers and TaqMan® probes specific for both mutant and wild-type DNA (Fig. 1a).

A Poisson distribution of gDNA is expected in the droplets and, assuming that the mass of a (haploid) genome equivalent is 3.3 pg, in an emulsion containing 100 μL of aqueous phase each droplet should contain, on average, 0.08 genome equivalents (for the 9 pL droplets) or 0.04 genome equivalents (for the 4 pL droplets). The probes specific for mutated sequences were conjugated to the fluorophore 6-FAM (6-carboxyfluorescein, λ_{ex} 494 nm/λ_{em} 522 nm), which generates a green-fluorescent signal, whereas the probe complementary to wild-type sequence was conjugated to the fluorophore NED (2,7′,8′-benzo-5′-fluoro-2′,4,7-trichloro-5-carboxyfluorescein, λ_{ex} 546 nm/λ_{em} 575 nm), which generates a red-fluorescent signal. The emulsion was thermocycled off-chip, in a specially adapted tube, using a conventional thermocycler (Fig. 1b). After thermocycling, the droplets were analyzed by injecting the emulsion onto a second microfluidic device, spacing the droplets with oil, and measuring the green and red fluorescence of each droplet in a microfluidic channel upon laser excitation (Fig. 1c). In addition, a monolayer of emulsion was analyzed by confocal microscopy. Red, green and yellow droplets were counted to evaluate the ratio of mutant to wild-type genes (Table 1 and Fig. 2).

For H358, LoVo, SW620 and SW48 cell-lines the ratio of fluorescent to non-fluorescent droplets was in the range of 0.06 to

Table 1 Mutant Allelic Specific Imbalance (MASI) analysis. Variations in the ratio of mutant to wild-type *KRAS* alleles (mA%) were determined in four heterozygous cell-lines (H1573, H358, LoVo, and LS123) and compared with literature data obtained by DNA sequencing (DNA seq.), restriction fragment length polymorphism (RFLP), subcloning or cDNA sequencing (cDNA seq.).[58] No literature data were available (NA) for the H1573 cell-line. The cell-lines SW48 and SW620, which are homozygous for wild-type and mutant *KRAS*, respectively, were used as controls

Cell-line	Mutation	Number of droplets analyzed	Number of droplets containing DNA			Experimental mA%	Reported mA%			
			Green droplets	Red droplets	Yellow droplets		DNA seq.	RFLP	Subcloning	cDNA seq.
SW48	—	11 490	0	1228	0	0	NA	NA	NA	NA
SW620	G12V	4938	621	0	0	100	NA	NA	NA	NA
H1573	G12A	5612	119	116	2	49.3	NA	NA	NA	NA
H358	G12C	4677	239	145	0	62.2	68.7	85.0	82.4	71.8
LoVo	G13D	28 905	2317	1134	34	67.1	66.7	NA	68.4	NA
LS123	G12S	23 192	336	330	9	50.4	60.3	51.3	55.0	NA

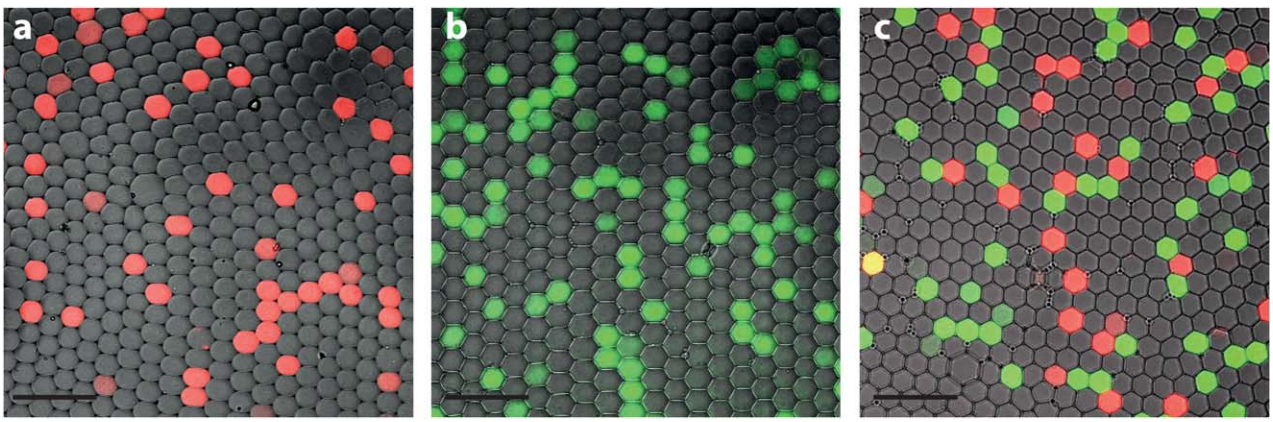

Fig. 2 Fluorescence confocal microscopy analysis of thermocycled droplets. gDNA extracted from homozygous cell-lines bearing wild-type *KRAS* alleles (SW48) (a), mutant *KRAS* alleles (SW620) (b) and a heterozygous cell-line bearing both mutant and wild-type *KRAS* alleles (H358) (c) were analyzed by fluorescence confocal microscopy. TaqMan® probes specific for the wild-type sequence carried a NED fluorophore (λ_{ex} 546 nm/λ_{em} 575 nm) and TaqMan® probes specific for the mutant sequences carried a 6-FAM fluorophore (λ_{ex} 494 nm/λ_{em} 522 nm). Red-fluorescent droplets contain wild-type DNA, green-fluorescent droplets contain mutant DNA, yellow-fluorescent droplets contain both mutant and wild-type DNA, and non-fluorescent droplets do not contain target DNA (scale bar 100 μm).

0.1, consistent with the expected number of *KRAS* genes per droplet (0.08) (Table 1 and Fig. 2). For LS123 and H1573 cell-lines, on the other hand, this ratio was in the range of 0.03 to 0.04, consistent with the expected number of *KRAS* genes per droplet (0.04). As expected, with gDNA from the homozygous cell-line containing a wild-type *KRAS* gene (SW48) all fluorescent droplets were red (Fig. 2a and Table 1) and with the homozygous cell-line containing a mutated *KRAS* gene (SW620) all fluorescent droplets were green (Fig. 2b and Table 1). For the four different heterozygous cell-lines containing a mutated and a wild-type *KRAS* gene (H1573, H358, LoVo and LS123), the fluorescent droplets were either red (due to amplification of a wild-type *KRAS* gene), green (due to amplification of a mutant *KRAS* gene), or yellow (due to amplification of a mutant and a wild-type *KRAS* gene) (Fig. 2c and Table 1).

Variations in the ratio of mutant to wild-type alleles (mutant allele specific imbalances or MASI) are commonly observed in tumors and cell-lines harboring oncogenic mutations, and have been described for various oncogenes, including *KRAS*.[52] The ratios of mutant to wild-type *KRAS*, determined for the heterozygous cell-lines H358, LoVo and LS123 from the ratio of green to red droplets, were in good agreement with previously published data for the same cell-lines (Table 1).[52]

Quantification of mutated and wild-type *KRAS* DNA: determination of the sensitivity of the procedure

To demonstrate that genes bearing a somatic mutation can be detected within a large excess of wild-type sequences, gDNA from the heterozygous cell-line H1573, which contains a G to C transversion in the second base of *KRAS* codon 12, was serially diluted into gDNA containing the wild-type *KRAS* gene from the cell-line SW48. The gDNA was fragmented by nebulization to obtain 1–5 kb fragments. This not only approximates the situation with clinical samples such as plasma where the DNA is degraded to small fragments by nucleases[53] but also decreases viscosity, an essential condition for rapid and stable droplet generation. The DNA mixtures were diluted to 30 ng μL^{-1}, and compartmentalized in 9 pL droplets, together with PCR reagents, primers and TaqMan® probes specific for both mutant and wild-type DNA and processed as above (Fig. 1). The ratio of green to red fluorescent droplets in gDNA from the cell-line

H1573 alone indicates a mutant allelic fraction of 49% (Table 1). The ratio of mutant to wild-type *KRAS* was then determined from the ratio of green to red droplets in 10-fold serial dilutions of H1573 gDNA in wild-type SW48 gDNA (Fig. 3). There was a close linear correlation (coefficient of determination, $R^2 > 0.99$) between the theoretical and experimental ratio of mutant *KRAS* to wild-type *KRAS* down to 1 mutant in 200 000 wild-type *KRAS* genes. The method is thus, both sensitive and quantitative, the sensitivity being limited only by the number of droplets analyzed. By analyzing ~10^6 fluorescent droplets, even the results obtained for the highest dilution (1/200 000) fall within the 95% confidence interval, though the results were less precise than for lower dilutions due to the limited number of green droplets (corresponding to mutated genes) analyzed: the maximum number of green droplets observed in a single experiment was 16 (within 1 871 215 red droplets). To obtain more precise data for high dilutions, a greater number of droplets could be analyzed (Fig. S2†). The number of fluorescent droplets that need to be analyzed to achieve a desired sensitivity can be determined by calculating the threshold at which finding no green-fluorescent (mutant) droplets is within the 95% confidence interval. When the number of green-fluorescent droplets containing mutant DNA, N_g, is much smaller than the total number of red-fluorescent droplets containing wild-type DNA, N_r, and the total number of droplets, N, the 95% confidence interval is in good approximation:

$$F = F^*\left(1 \pm \frac{1.96}{\sqrt{N_m}}\right) \quad (1)$$

where $F = N_g/N_r$ and $F^* = N_m/N_{wt}$ = ratio of mutant to wild-type genes (see ESI†). Solving eqn (1) for $F > 0$ and $N_{wt}/N = 0.1$ we obtain $N > 1.96^2/(0.1\ F^*)$. For example, when $F^* = N_m/N_{wt} = 5 \times 10^{-6} = 1/200\,000$, to exclude $N_m = 0$ from the 95% confidence interval more than 7 683 200 droplets should be analyzed ($1.96^2/(0.1 \times 5 \times 10^{-6})$). Reciprocally, if we measure $N_m = 0$ we can say that $F^* < 1.96^2/0.1N$ within the 95% confidence limit. The threshold N_m/N_{wt} of 3.84×10^{-5} at which $N_m = 0$ falls in the 95% confidence interval for $N = 10^6$ and $N_{wt}/N = 0.1$ is indicated in Fig. 3.

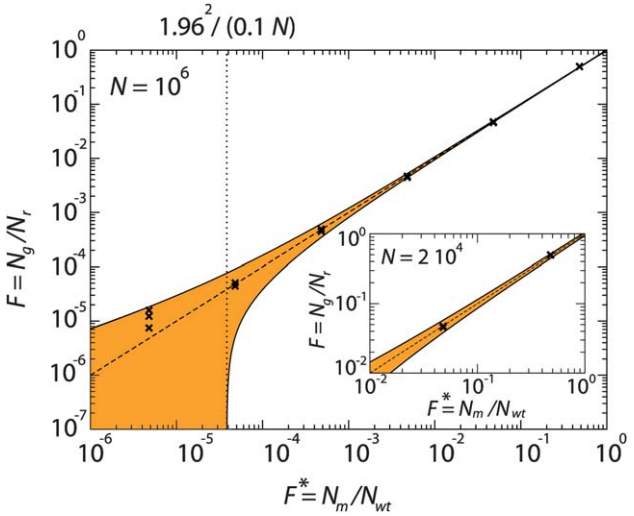

Fig. 3 Sensitivity of the method. Experimental measurement of the fraction of green-fluorescent droplets containing mutant *KRAS* (N_g) over the number of red-fluorescent droplets containing wild-type *KRAS* (N_r) as a function of the ratio of mutant (N_m) to wild-type (N_{wt}) genes. In an ideal assay, N_g/N_r is equal to N_m/N_{wt} (dashed line). The 95% confidence interval (orange area) for the analysis of $N = 10^6$ droplets when $N_{wt}/N = 0.1$ is shown (see ESI† for details on the determination of the 95% confidence interval). All the experimental points (×) obtained in duplicate (except for the 1/200 000 which was in triplicate) for the different dilutions fall into this 95% confidence interval. The dotted line corresponds to the point where a measured $N_m = 0$ falls in the 95% confidence interval. Inset: higher ratios of mutant to wild-type genes, statistically relevant data are obtained by the analysis of a smaller subset of droplets. The experimental points (×) are plotted as a zoom and compared to the 95% confidence interval (orange area) determined from the analysis of $N = 2 \times 10^4$ droplets analyzed experimentally.

Parallel analysis of multiple mutations in *KRAS*

We have adapted the method to simultaneously detect and quantify multiple somatic mutations in a single experiment (Fig. 4). First, a microfluidic device was used to produce a "probe emulsion" comprising seven different types of 3 pL droplets (Fig. 4a and S1a†). Each type of droplets contained a TaqMan® probe, labeled with 6-FAM, targeting the six most common mutations in codon 12 of the *KRAS* gene, or the wild-type *KRAS* codon 12.[54]

In addition, each type of droplets contained a different concentration of a red fluorescent dye (Dextran Texas Red, DTR), which served as a code to identify the *KRAS* sequence targeted by the probe in each droplet. The droplets were pooled, then re-injected onto a microfluidic device where they were spaced by oil and passively fused one-to-one with 9 pL droplets produced on-chip containing PCR reagents and gDNA (Fig. 4b and S1b†). We used a passive droplet fusion device which does not require any electric fields, lasers or specific channel treatment to induce droplet fusion:[55] the fusion chip is therefore simple to use and manufacture, requiring no electrodes or surface patterning. Using a ~7 : 2 ratio of 3 pL : 9 pL droplets ~60% of 9 pL droplets were fused with a single 3 pL droplet.

The emulsion obtained after fusion was thermocycled and the fluorescence of each droplet measured as described above (Fig. 1). As a proof of principle for this strategy we analyzed 12 μg of gDNA from the heterozygous cell-line H1573, which contains a nearly 1 to 1 ratio *KRAS* genes with a G to C transversion in the second base of codon 12 and wild-type *KRAS* genes. Fig. 5 shows the results obtained with this strategy. Plotting red fluorescence *versus* droplet width allowed droplets containing the seven different probes to be identified and droplets arising from uncontrolled coalescence to be excluded from subsequent analysis (Fig. 5a). The apparent droplet width increases with increasing red fluorescence[56] therefore separate width gates were defined for each population. The red and green fluorescence of the gated droplets was then plotted (Fig. 5b). Two populations of green-fluorescent droplets were identified, corresponding to droplets containing TaqMan® probes for wild-type codon 12 and the G to C transversion in the second base of codon 12: 7.6% of droplets with the wild-type code were green-fluorescent, 8.0% of droplets with the code for the G to C transversion of codon 12 were green-fluorescent. This corresponds to

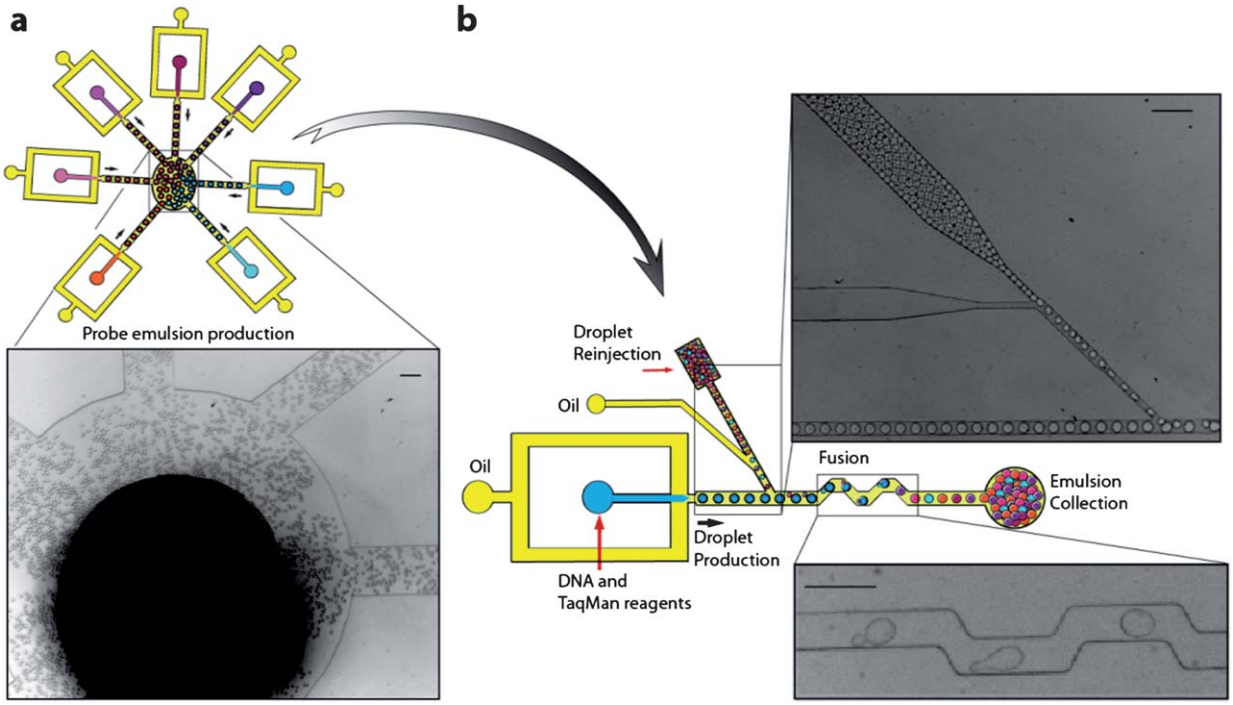

Fig. 4 Parallel analysis of multiple mutations. (a) A device capable of producing seven different types of droplets—each containing a different TaqMan® probe that targeted either the wild-type or one of the six most common mutations in codon 12 of the *KRAS* oncogene—was used to generate a probe emulsion. In addition, each type of droplets contained a different concentration of a red-fluorescent dye (Dextran Texas Red, DTR). The pooled droplets were collected off-chip and reinjected onto a passive fusion device (b) where they were fused one-to-one with droplets produced on-chip containing all PCR reagents and gDNA. Light micrographs of probe emulsion production and re-injection, as well as droplet fusion are shown (scale bar, 100 μm). The fused emulsion was collected in a PDMS-sealed tube (collection/reinjection device), thermocycled and then reinjected for on-chip droplet fluorescence analysis (see Fig. 1).

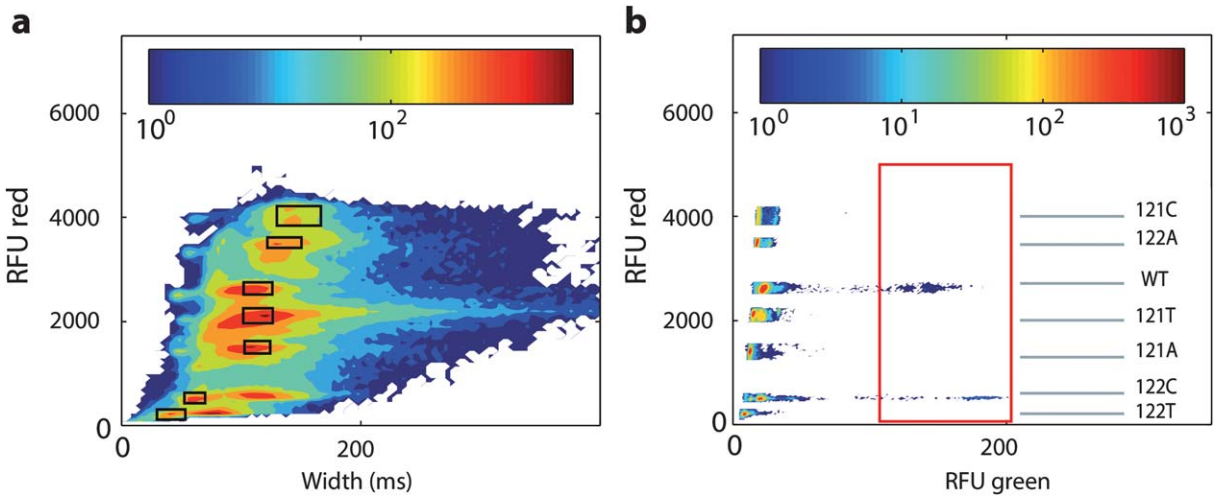

Fig. 5 Parallel multiple mutation analysis. The emulsion obtained after fusion of the probe emulsion with droplets produced on-chip containing target DNA (see Fig. 4) was reinjected for fluorescence analysis. For each droplet, in the red channel, the peak width (droplet size) and maximum peak fluorescence (DTR code) were recorded, and in the green channel, the maximum peak fluorescence (TaqMan® probe signal) was recorded. (a) Plotting red fluorescence *versus* droplet width (time for droplet to pass through the laser spot in ms) allowed identification of the droplets containing the 7 different probes and gating (black boxes) to eliminate artefactual data due to uncontrolled droplet coalescence while thermocycling or non-fused droplets from the probe emulsion (27% of droplets gated). (b) The data from the gated droplets were replotted as red fluorescence *versus* green fluorescence. Greater than 98% of all green fluorescent droplets (red box) corresponded to droplets containing TaqMan® probes for mutant DNA bearing a heterozygous *KRAS* mutation of G to C transversion on the second base of codon 12 (122C) and droplets containing TaqMan® probes for wild-type DNA (WT) at a nearly equal ratio (mA% = 51%). The graph in (a) contains 50 000 bins (500 for the RFU red axis and 100 for the width axis) and the graph in (b) contains 150 000 bins (500 for the RFU red axis and 300 for the RFU green axis). The color code indicates the number of droplets per bin.

a mutant allelic fraction (mA%) of 51%, very close to the expected value of 49.3% (Table 1). Only 1.75% of all other populations contained green fluorescent droplets.

Discussion

We demonstrate a droplet-based microfluidic system, based on digital PCR, which enables highly sensitive, specific and quantitative detection of somatic mutations in target genes in gDNA. We used a dual-probe TaqMan® assay to quantify mutations in the *KRAS* oncogene. These probes, previously validated clinically in conventional (bulk) microplate systems,[15,54] allow the ratio of mutant to wild-type alleles to be determined from the ratio of green to red fluorescence. They have been developed to detect *KRAS* mutations within tumoral samples from patients with metastatic colorectal cancer before treatment with anti-epidermal growth factor receptor (EGFR) antibodies (Cetuximab and Panitumumab). Indeed, the presence of any of these mutations has been found to be one of the most relevant predictive markers of responses to therapy with anti-EGFR antibodies.[57,58] However, in bulk, the sensitivity of these probes on gDNA is only 10% (1 mutant gene in 10 wild-type genes)[15] and they are not sufficiently sensitive to allow analysis of clinical samples like stool or plasma where tumor derived DNA fragments represent only a small fraction of the total DNA.[20]

However, we show here that by compartmentalizing the same TaqMan® probes in picolitre droplets together with, on average, less than one (haploid) genome equivalent of gDNA per droplet, the sensitivity can be improved by at least a factor of $\sim 10^4$: by analyzing $\sim 10^6$ fluorescent droplets we could quantify DNA down to 1 mutant *KRAS* gene in 200 000 wild-type *KRAS* genes. This level of sensitivity is sufficiently high to enable the detection of circulating DNA from early stage tumors in plasma.[30] For example, it has been reported that for patients with early colorectal cancer, mutant *APC* (*adenomatous polyposis coli*) sequences could be detected at levels ranging from 0.01 to 1.7% of the total *APC* molecules present in plasma.[30]

Indeed, the sensitivity of the system is only limited by the number of genes that can be analyzed. This is a function of the rate at which droplets can be created and screened ($\sim 10^6$ droplets per hour) and, λ, the average number of target genes per droplet (0.1), *i.e.* $\sim 10^5$ genes per hour. The number of genes analyzed per hour could be increased by increasing λ to 1, thereby maximizing the number of droplets containing single genes, and fitting the number of green, red, yellow and non-fluorescent droplets to a Poisson distribution. Furthermore, the rate limiting step is currently re-injection of droplets for fluorescence measurement, which could be increased, for example by parallelization.[59]

Sensitivity can also be limited by the amount of DNA in patient samples. Indeed, the concentration of free circulating DNA in plasma is generally a few nanograms per millilitre for healthy subjects and can increase significantly in patients with cancer (10–1200 ng mL^{-1}).[60–62] Such DNA concentrations lead to $\sim$3000 to 360 000 target genes per mL of plasma. Within this limit, we are already able to accurately detect any mutant DNA within a given sample (if mutant DNA is present within the sample). The target gene could potentially be pre-amplified before compartmentalization in droplets, but this would negate one of the major advantages of this, and other digital amplification techniques, *i.e.* the sensitivity is not limited by the DNA polymerase error rate. Even if an error occurs in the first cycle of PCR, this will result in a mutant to wild-type ratio of one to three. This translates to a mixed mutant/wild-type signal and can be excluded from the calculation.

Compared to the original microplate-based digital PCR systems, whose use for highly sensitive detection was limited by reagent cost and time, the volume of reagents required (for the same sensitivity) is reduced by $\sim 10^6$-fold (reaction volume drops from μL to pL) and the time reduced by $\sim 10^3$-fold (analysis speed is increased from Hz to kHz). Compared to digital PCR in microfluidic systems with compartments defined by pneumatic valves, or in nanolitre volume droplets, the volume of reagents required for each reaction is reduced by $\sim 10^3$-fold (reaction volume drops from nL to pL) and the time reduced by $\sim 10^3$-fold (analysis speed is increased from Hz to kHz). Millions of individual DNA fragments can be analyzed by BEAMing, in which single DNA molecules are amplified by PCR on beads in femtolitre volume droplets in emulsions and then analyzed using flow cytometry.[26,27] This digital amplification procedure is highly sensitive and has been used to quantify mutated DNA circulating in the plasma of colorectal cancer patients.[30] However, in contrast to the droplet-based microfluidic approach described here, BEAMing requires pre-amplification of the plasma DNA.[26,63] In addition, BEAMing requires the emulsion to be broken and beads processed to fluorescently tag the different alleles before analysis using flow cytometry. In contrast, with digital PCR in droplet-based microfluidic systems the target DNA is amplified and detected directly in the droplets, and the procedure is performed entirely in disposable, single-use devices, decreasing the time to process each sample, and reducing the risk of cross-contamination. In the future, it should be possible to further simplify the system by using a single integrated microfluidic chip to make droplets, thermocycle, either by thermocycling the entire chip[45] or by passing the droplets between different temperature zones,[39,41] and measure droplet fluorescence.

We have also demonstrated that, by one-to-one fusion of drops containing gDNA with any one of the seven different types of droplets, each containing a TaqMan® probe specific for a different *KRAS* mutation or wild-type *KRAS*, and an optical code,[64] it was possible to screen the six common mutations in codon 12 of *KRAS* in parallel in a single experiment. This procedure has similarities with that previously developed for microdroplet-based PCR enrichment for large scale targeted sequencing.[65] In the system described here, however, the emulsion libraries comprise droplets which contain different TaqMan® probes, rather than different primer-pairs, and the fusion of these droplets with droplets containing gDNA and PCR reagents is achieved without the use of external electric fields.[55]

The accompanying manuscript[66] describes another approach to simultaneously analyze multiple markers using digital PCR in a droplet-based microfluidic system. This alternative system allows multiplexing of digital PCR in picolitre droplets and was used to study the congenital disease spinal muscular atrophy (SMA). A 5-plex assay with just two fluorophores was demonstrated to simultaneously measure the copy number of two genes implicated in SMA (SMN1 and SMN2) and to genotype a single nucleotide polymorphism (c.815A > G, SMN1). Accurate and precise copy numbers of up to sixteen per cell were measured

using a model system and the results of a pilot study with SMA patients are presented. Within the limits imposed by spectral overlap of fluorophores it would be possible to envisage combining both the droplet fusion approach described herein and the multiplex approach to analyse large numbers of markers in a single experiment.

The high sensitivity and precision of digital PCR in droplet-based microfluidic systems should enable the screening and diagnosis of cancer using DNA from easily accessible patient samples such as plasma, urine and stool. Furthermore, it can provide valuable data to aid in clinical management, by allowing the detection of residual disease and relapse, and for personalized medicine.

For example, *KRAS* mutations have been strongly linked to resistance of colorectal tumors to antibody-based treatment targeting the epidermal growth factor receptor (EGFR). However, it has recently been pointed out that, in colorectal cancer, when the frequency of *KRAS* mutations in clinical samples is low (<20%) some patients still respond to anti-EGFR antibodies.[67] Prospective studies using highly sensitive procedures are needed to evaluate the role of different percentages of mutated alleles in response to anti-EGFR treatment in larger numbers of patients. We believe that the quantitativity and sensitivity offered by our procedure could allow the identification of reproducible thresholds of *KRAS* mutations which confer resistance to anti-EGFR drugs which can be used by clinicians to guide their therapeutic strategy.[68]

We believe that this system has many potential applications beyond clinical oncology. The high sensitivity of the procedure could allow, for example, the detection of infectious diseases or prenatal identification of foetal alleles in maternal blood.[69,70] Extensions of the procedure could also find applications in the detection of gene copy number amplifications; a feature associated with susceptibility or targeted treatment resistance in many diseases including cancers.[71] Moreover, the large dynamic range of at least 5 orders of magnitude should make it a powerful tool for the quantitative analysis of transcription.

Experimental

gDNA preparation

Cell-lines bearing wild-type or mutant *KRAS* alleles were purchased from the American Type Culture Collection (ATCC, LGC, Molsheim, France): SW48 (ATCC CCL-231, wild-type DNA), H358 (ATCC CRL-5807, transversion G to T in the first base of *KRAS* codon 12, G12C), LS123 (ATCC CCL-255, transition G to A in the first base of *KRAS* codon 12, G12S), SW620 (ATCC CCL-227, transversion G to T in the second base of *KRAS* codon 12, G12V), H1573 (ATCC CRL-5877, transversion G to C in the second base of *KRAS* codon 12, G12A), and LoVo (ATCC CCL-229, transition G to A in the second base of *KRAS* codon 13, G13D). gDNA was extracted from cultured cells using a QIAamp DNA mini Kit (Qiagen, Courtaboeuf, France). gDNA was eluted in sterile nuclease free water (Roth, Karlsruhe, Germany). Purified DNA was either used directly or first nebulized to obtain fragments ranging from 1–5 kb using a Nebulizer Kit (Invitrogen, Life Technologies corp., Villebon sur Yvette, France). DNA was precipitated according to the manufacturer's protocol and resuspended in 50 μL sterile nuclease free water. DNA concentration was determined by measuring the absorbance at 260 nm using a Nanodrop ND-1000 spectrophotometer (Thermo Scientific, Wilmington, USA). To estimate the sensitivity of the procedure, nebulized gDNA extracted from the H1573 heterozygous cell-line was diluted in nebulized wild-type gDNA extracted from the SW48 cell-line. The dilutions were performed from 1/10 to 1/100 000, leading to ratios of mutant/wild-type *KRAS* alleles from ~1/20 to ~1/200 000 (the initial fraction of the mutant allele in the H1573 cell-line is 49%).

Microfluidic device fabrication

The different microfluidic chips (Fig. S1†) were fabricated by patterning channels in poly(dimethylsiloxane) (PDMS) using soft lithography.[72] Briefly, SU8-2015 photoresist (MicroChem Corp., Newton, USA) was spin-coated onto silicon wafers (Siltronix, Archamps, France), patterned by UV exposure (MJB3 contact mask aligner; SUSS MicroTec, Lyon, France) through a photolithography mask and then developed (SU-8 developer; MicroChem Corp.). The thickness of the photoresist was 25 μm to make devices for sensitivity tests and 20 μm for all other devices. Then a 10 : 1 (w/w) mixture of Sylgard 184 silicone elastomer and curing agent (Dow Corning Corp., Michigan, USA), degassed under vacuum, was poured onto the silicon wafer to a depth of 5 mm and cured at 65 °C for 2 hours. After hardening, the PDMS was gently peeled from the master and input/output ports were punched out of the PDMS with a 0.75 mm diameter Harris Uni-Core biopsy punch. Particles of PDMS were cleared from the ports using pressurized nitrogen gas. The structured side of the PDMS was bonded to a 76 × 26 × 1 mm glass microscope slide (Paul Marienfeld GmbH & Co. KG, Lauda-Königshofen, Germany) by exposing both parts to an oxygen plasma (Diener Electronic, Ebhausen, Germany) and pressing them together. Finally, a hydrophobic surface coating was applied to the microfluidic channel walls by injecting 2% perfluorooctyldimethylsilane (Aldrich, Sigma-Aldrich Chimie S. a.r.l., Lyon, France) in HFE-7100 oil (3M, St Paul, USA). Excess fluorosilane was rinsed from the device using pure HFE-7500 oil.

Emulsification of TaqMan® reactions

The TaqMan® MGB probes (Applied Biosystems, Life Technologies corp., Villebon sur Yvette, France) and the primers allowing amplification of the *KRAS* target sequences were previously developed and validated for clinical sample analysis.[54] The probes specific for mutated sequences are conjugated to the fluorophore 6-FAM (λ_{ex} 494 nm/λ_{em} 522 nm) whereas the probes complementary to wild-type sequence are conjugated to the fluorophore NED (λ_{ex} 546 nm/λ_{em} 575 nm). A 200 μL PCR reaction was set up containing: detergent-free buffer; 200 μM dNTPs (MP Biomedicals); 0.3 μM forward primer; 0.3 μM reverse primer (Eurogentec, Angers, France); 200 nM TaqMan® probe specific of mutant sequence; 750 nM TaqMan® probe specific of wild-type sequence; 5 units of DyNAzyme II polymerase (5 U μL^{-1}, Finnzymes, Espoo, Finland).

The aqueous solution was placed in a 1 mL polyethylene syringe (Omnifix-F®, BBRAUN, Bad Arolsen, Germany) with

a 23G syringe needle and injected into the microfluidic device using 0.56 mm × 1.07 mm polytetrafluoroethylene (PTFE) tubing. Fluorinated oil (HFE-7500, 3M) containing 2% (w/w) EA-surfactant (a PEG–PFPE amphiphilic block copolymer[73]) was placed in a 1 mL syringe. The aqueous phase was injected at 100 μL h^{-1} and the oil phase at 200 μL h^{-1} using syringe pumps (PHD 2000, Harvard Apparatus, Les Ulis, France) and 10 pL droplets were generated on-chip by hydrodynamic flow-focusing[74] (a production frequency of 30 kHz).

Thermocycling in emulsion droplets

The emulsion generated in the microfluidic devices was collected in a 'collection/reinjection' device (Fig. 1). The collection/reinjection device was made of a PCR tube (0.5 mL, Thermo Fisher Scientific, Illkirch, France) sealed by a PDMS plug in which two holes were punched (0.75 mm diameter biopsy punch), and into which the inlet and outlet tubing (0.56 mm × 1.07 mm PTFE tubing) was inserted using tweezers. After removal of the tubing, the device containing the emulsion was placed in a PCR Machine (Mastercycler®, Eppendorf, Le Pecq, France) and the emulsion was thermocycled, starting with an initial denaturation step of 2 min at 94 °C, followed by 39 cycles of: 94 °C, 15 s and 60 °C, 1 min.

On-chip droplet fluorescence analysis

The thermocycled emulsion was reinjected into a second microfluidic device for fluorescence measurement. Droplets were reloaded at a flow rate of 50 μL h^{-1} (a droplet reinjection frequency of 268 Hz) and spaced by HFE-7500 oil with no surfactant flowing at a rate of 100 μL h^{-1}. This procedure enabled droplets to be well separated in a 20 μm wide and 20 μm deep channel for fluorescence analysis. Spacing of the emulsion for reinjection was necessary since droplets cream during thermocycling.

The fluorescence of each droplet was measured using the optical set-up (described in ref. 75) comprising a 488 nm (CYAN-20-C, Picarro, BFi OPTiLAS, Evry, France) and a 532 nm (Excelsior 532-20-C, Spectra-Physics, Evry, France) lasers, with photomultiplier tubes (PMTs) (Hamamatsu Photonics, Japan) measuring fluorescence at 510 ± 10 nm (green) and 617 ± 36.5 nm (red). For each droplet the maximum intensity of the droplet fluorescence peak was recorded as well as the width of the peak, corresponding to the droplet size. The PMTs return a voltage U, which is a function of the gain G applied to the PMT. In order to compare values of U obtained for different gains, we defined the Relative Fluorescence Unit (RFU) as $RFU = U/G^{7.2}$ with U and G expressed in volts. The exponent 7.2 was given by the PMT manufacturer and has been confirmed experimentally.

Data acquisition and data processing

Data acquisition (DAQ) of the PMT signal was performed by a PCI-7831R Multifunction Intelligent DAQ executing a program written in LabView 8.2 (National Instruments Corporation, Nanterre, France). The data acquisition rate for the system was 100 kHz. The green and red fluorescence of each droplet was recorded as well as droplet width. Data were processed and plotted, using a homemade Matlab code. The measurement of the droplet width enabled droplets of unexpected size (due to uncontrolled coalescence or splitting) to be removed from the analysis and, in the experiments using controlled pairwise droplet fusion, to distinguish fused and unfused droplets.

When using a single TaqMan® probe the concentration of target DNA is determined by fitting the fraction of fluorescent droplets, Z (which contain ≥1 target DNA molecule), to the Poisson distribution (eqn (2)).

$$p_k = \frac{\lambda^k e^{-\lambda}}{k!} \tag{2}$$

The probability p_k to encapsulate k genes in one droplet depends on the average number of genes per droplet λ and the fraction of fluorescent droplets is:

$$Z = 1 - e^{-\lambda} \tag{3}$$

When using a pair of TaqMan® probes specific for mutant and wild-type genes which generate green-fluorescent (mutant) and red-fluorescent (wild-type) signals, the ratio of mutant, N_m, to wild-type genes, N_{wt}, genes can be determined from eqn (4).

$$\frac{N_m}{N_{wt}} = \frac{\lambda_m}{\lambda_{wt}} = \frac{-\ln(1 - Z_m)}{-\ln(1 - Z_{wt})} = \frac{-\ln\left(1 - (N_g + N_y)/N\right)}{-\ln\left(1 - (N_r + N_y)/N\right)} \tag{4}$$

where λ_m and λ_{wt} are the mean number of mutant and wild-type DNA molecules per droplet, respectively; Z_m and Z_{wt} are the number of fluorescent droplets corresponding to amplification of the mutant and wild-type probes, respectively; N_g is the number of green droplets, N_r the number of red droplets, N_y the number of yellow droplets (*i.e.* both green and red) and N the total number of droplets.

However, when λ_m and λ_{wt} are less than 0.1, as in all experiments herein, the ratio of mutant, N_m, to wild-type genes, N_{wt}, genes can be determined, from eqn (5), and can be determined, to close approximation, simply from the ratio green to red droplets, N_g/N_r. Indeed, the error resulting from this approximation is less than λ at all ratios of N_m/N_{wt} and tends to λ as N_m/N_{wt} tends to zero.

$$\frac{N_m}{N_{wt}} = \frac{\lambda_m}{\lambda_{wt}} \approx \frac{Z_m}{Z_{wt}} \approx \frac{N_g}{N_r} \tag{5}$$

Fluorescence microscopy

The emulsion was spread between two 0.17 mm thick microscope coverslips and images were acquired with LSM510 laser-scanning confocal microscope (Zeiss, Jena, Germany) equipped with C-Apochromat 20× (n.a. 0.8) water immersion objectives in multitrack mode. The 6-FAM fluorophore was excited at 488 nm using an argon laser, and the emission spectra were recorded in the range 505–550 nm. The NED fluorophore was excited using a helium–neon 561 nm laser and the emission spectra were recorded beyond 585 nm. Images were processed with Zeiss LSM Image Browser, version 4.0SP1, software and with ImageJ 1.42q (National Institutes of Health, USA) to obtain composites.

Parallel multiple mutation analysis

A microfluidic device (Fig. 4 and S1†) was used to simultaneously produce seven different types of 3 pL droplets

(the "probe emulsion") by flow-focusing of seven different aqueous phases with HFE-7500 oil containing 2% (w/w) EA-surfactant. Each aqueous phase comprised detergent-free buffer containing a TaqMan® MGB probe (800 μM), labeled with 6-FAM, targeting one of the six common mutations in codon 12 of the *KRAS* oncogene, or the wild-type *KRAS* codon 12.[54] The droplets were collected off-chip in a syringe and then re-injected into a microfluidic device where they were spaced by HFE-7500 oil and fused one-to-one with 9 pL droplets produced on-chip (at 1.7 kHz) with HFE-7500 oil containing 0.5% (w/w) EA-surfactant (Fig. 4 and S1†).[55] These droplets contained the target DNA; detergent-free buffer; 200 μM dNTPs; 0.3 μM forward primer; 0.3 μM reverse primer (Eurogentec) and 5 units of DyNAzyme II polymerase. The emulsion obtained after fusion was thermocycled as described above (Fig. 1). 12 μg of DNA from the non-nebulized heterozygous cell-line H1573 was used as target DNA.

Efforts to minimize contamination

To minimize contamination by exogenous DNA, all DNA manipulations prior to amplification were performed in a UV-treated environment (Biocap DNA/RNA hood, Fisher Bioblock Scientific, Illkirch, France). The TaqMan® probes were aliquoted upon arrival and stored at −20 °C. A new aliquot was used for each set of experiments. Dilutions of PCR reagents and dyes were performed in sterile DNase-, RNase-free, DEPC-treated water (Roth, Karlsruhe, Germany). A new device was used for each set of experiments, going from the more diluted to the more concentrated DNA sample to limit carry-over effects. In addition, all the experiments were carried out using certified DNA-free, sterilized, filtered pipette tips. Disposable tweezers (Roth, Karlsruhe, Germany) were used for microfluidic experiments. All disposables (tweezers, PCR tubes, collection-reinjection devices, tubing, *etc.*) were UV-irradiated before use. Nebulization of gDNA was performed under chemical hoods in physically separated rooms.

Conclusions

We have developed a highly sensitive, quantitative procedure to measure the ratio of mutant and wild-type genes in gDNA using a droplet-based microfluidic system to perform digital TaqMan® assays. Millions of droplets are created, each containing, on average, less than one target gene and two TaqMan® probes, one specific for the mutant and the other for the wild-type DNA, which generate green and red fluorescent signals, respectively. After thermocycling, the ratio of mutant to wild-type genes is determined by counting the ratio of green to red droplets. This digital procedure allowed the determination of mutant allelic specific imbalance (MASI) in several cancer cell-lines and the precise quantification of a mutated *KRAS* oncogene in the presence of a 200 000-fold excess of unmutated *KRAS* genes in gDNA. The sensitivity is, therefore, much higher than conventional, bulk, TaqMan® assays, which cannot detect less than ~1% mutant *KRAS* in a background of non-mutated DNA from normal cells. Furthermore, by creating optically encoded droplets containing TaqMan® probes specific for different *KRAS* mutations, or wild-type *KRAS*, it was possible to screen six of the most common mutations *KRAS* (all in codon 12) in parallel in a single experiment. An alternative approach to simultaneously analyze multiple markers, based on multiplexing of digital PCR in picolitre droplets is described in the accompanying manuscript[66] and was used to measure gene copy number variations in the congenital disease spinal muscular atrophy (SMA). Together, these papers show that digital genetic testing using droplet-based microfluidics should allow the characterization of clinical samples for various genetic alterations including rare somatic mutations and gene copy-number variations. We believe it has many potential applications, including in clinical oncology, for the diagnosis, prognosis, treatment and follow-up of patients, where tumor-specific somatic mutations must frequently be detected and quantified in a large excess of non-mutated DNA from normal cells.

Acknowledgements

Deniz Pekin and Yousr Skhiri were supported by the Région Alsace. This work was supported by the Ministère de l'Enseignement Supérieur et de la Recherche, the Université de Strasbourg, the Université Paris Descartes, the Centre National de la Recherche Scientifique (CNRS), the Institut National de la Santé et de la Recherche Médicale (INSERM), the Institut National du Cancer (INCa, no. 2009-1-RT-03-US-1) and the Association pour la recherche sur le Cancer (ARC, no. SL220100601375). JC-B has been supported by a European Molecular Biology Organization (EMBO) long-term fellowship and the European Commission Framework Programme 6 (EC FP6) MiFem Network. The authors are grateful to Christian Rick and Estelle Mayot for help and assistance. We thank Alex Garvin (Droplet Diagnostics), Fabienne Mathon (Université de Strasbourg) and Olivier Guyot (Region Alsace) for helpful discussions.

Notes and references

1 B. Vogelstein and K. W. Kinzler, *Nat. Med.*, 2004, **10**, 789–799.
2 M. R. Stratton, P. J. Campbell and P. A. Futreal, *Nature*, 2009, **458**, 719–724.
3 F. Diehl and L. A. Diaz, Jr, *Curr. Opin. Oncol.*, 2007, **19**, 36–42.
4 C. L. Sawyers, *Nature*, 2008, **452**, 548–552.
5 T. Lecomte, A. Berger, F. Zinzindohoue, S. Micard, B. Landi, H. Blons, P. Beaune, P. H. Cugnenc and P. Laurent-Puig, *Int. J. Cancer*, 2002, **100**, 542–548.
6 J. Li, L. Wang, H. Mamon, M. H. Kulke, R. Berbeco and G. M. Makrigiorgos, *Nat. Med.*, 2008, **14**, 579–584.
7 C. A. Milbury, J. Li and G. M. Makrigiorgos, *Clin. Chem.*, 2009, **55**, 632–640.
8 C. M. Strom, *Mutat. Res.*, 2005, **573**, 160–167.
9 C. A. Foy and H. C. Parkes, *Clin. Chem.*, 2001, **47**, 990–1000.
10 D. Whitcombe, C. R. Newton and S. Little, *Curr. Opin. Biotechnol.*, 1998, **9**, 602–608.
11 G. Mike Makrigiorgos, *Hum. Mutat.*, 2004, **23**, 406–412.
12 P. Carotenuto, C. Roma, A. M. Rachiglio, F. Tatangelo, C. Pinto, F. Ciardiello, O. Nappi, R. V. Iaffaioli, G. Botti and N. Normanno, *Pharmacogenomics*, 2010, **11**, 1169–1179.
13 S. Dufort, M. J. Richard and F. de Fraipont, *Anal. Biochem.*, 2009, **391**, 166–168.
14 S. Ogino, T. Kawasaki, M. Brahmandam, L. Yan, M. Cantor, C. Namgyal, M. Mino-Kenudson, G. Y. Lauwers, M. Loda and C. S. Fuchs, *J. Mol. Diagn.*, 2005, **7**, 413–421.
15 A. Lievre, J. B. Bachet, V. Boige, A. Cayre, D. Le Corre, E. Buc, M. Ychou, O. Bouche, B. Landi, C. Louvet, T. Andre, F. Bibeau, M. D. Diebold, P. Rougier, M. Ducreux, G. Tomasic, J. F. Emile, F. Penault-Llorca and P. Laurent-Puig, *J. Clin. Oncol.*, 2008, **26**, 374–379.

16 B. Angulo, E. Garcia-Garcia, R. Martinez, A. Suarez-Gauthier, E. Conde, M. Hidalgo and F. Lopez-Rios, *J. Mol. Diagn.*, 2010, **12**, 292–299.
17 A. C. Tsiatis, A. Norris-Kirby, R. G. Rich, M. J. Hafez, C. D. Gocke, J. R. Eshleman and K. M. Murphy, *J. Mol. Diagn.*, 2010, **12**, 425–432.
18 P. J. Sykes, S. H. Neoh, M. J. Brisco, E. Hughes, J. Condon and A. A. Morley, *BioTechniques*, 1992, **13**, 444–449.
19 B. Vogelstein and K. W. Kinzler, *Proc. Natl. Acad. Sci. U. S. A.*, 1999, **96**, 9236–9241.
20 F. Diehl, K. Schmidt, K. H. Durkee, K. J. Moore, S. N. Goodman, A. P. Shuber, K. W. Kinzler and B. Vogelstein, *Gastroenterology*, 2008, **135**, 489–498.
21 S. M. Dong, G. Traverso, C. Johnson, L. Geng, R. Favis, K. Boynton, K. Hibi, S. N. Goodman, M. D'Allessio, P. Paty, S. R. Hamilton, D. Sidransky, F. Barany, B. Levin, A. Shuber, K. W. Kinzler, B. Vogelstein and J. Jen, *J. Natl. Cancer Inst.*, 2001, **93**, 858–865.
22 G. Singer, R. Oldt, 3rd, Y. Cohen, B. G. Wang, D. Sidransky, R. J. Kurman and M. Shih Ie, *J. Natl. Cancer Inst.*, 2003, **95**, 484–486.
23 I. M. Shih, H. Yan, D. Speyrer, B. M. Shmookler, P. H. Sugarbaker and B. M. Ronnett, *Am. J. Surg. Pathol.*, 2001, **25**, 1095–1099.
24 R. D. Mitra and G. M. Church, *Nucleic Acids Res.*, 1999, **27**, e34.
25 J. H. Leamon, W. L. Lee, K. R. Tartaro, J. R. Lanza, G. J. Sarkis, A. D. deWinter, J. Berka, M. Weiner, J. M. Rothberg and K. L. Lohman, *Electrophoresis*, 2003, **24**, 3769–3777.
26 D. Dressman, H. Yan, G. Traverso, K. W. Kinzler and B. Vogelstein, *Proc. Natl. Acad. Sci. U. S. A.*, 2003, **100**, 8817–8822.
27 M. Nakano, J. Komatsu, S. Matsuura, K. Takashima, S. Katsura and A. Mizuno, *J. Biotechnol.*, 2003, **102**, 117–124.
28 M. Li, F. Diehl, D. Dressman, B. Vogelstein and K. W. Kinzler, *Nat. Methods*, 2006, **3**, 95–97.
29 M. Nakano, N. Nakai, H. Kurita, J. Komatsu, K. Takashima, S. Katsura and A. Mizuno, *J. Biosci. Bioeng.*, 2005, **99**, 293–295.
30 F. Diehl, M. Li, D. Dressman, Y. He, D. Shen, S. Szabo, L. A. Diaz, Jr, S. N. Goodman, K. A. David, H. Juhl, K. W. Kinzler and B. Vogelstein, *Proc. Natl. Acad. Sci. U. S. A.*, 2005, **102**, 16368–16373.
31 H. L. Li, G. Xue and E. S. Yeung, *Anal. Chem.*, 2001, **73**, 1537–1543.
32 E. A. Ottesen, J. W. Hong, S. R. Quake and J. R. Leadbetter, *Science*, 2006, **314**, 1464–1467.
33 H. C. Fan and S. R. Quake, *Anal. Chem.*, 2007, **79**, 7576–7579.
34 S. L. Spurgeon, R. C. Jones and R. Ramakrishnan, *PLoS One*, 2008, **3**, e1662.
35 J. Qin, R. C. Jones and R. Ramakrishnan, *Nucleic Acids Res.*, 2008, **36**, e116.
36 T. K. F. Yung, K. C. A. Chan, T. S. K. Mok, J. Tong, K. F. To and Y. M. D. Lo, *Clin. Cancer Res.*, 2009, **15**, 2076–2084.
37 V. G. Oehler, J. Qin, R. Ramakrishnan, G. Facer, S. Ananthnarayan, C. Cummings, M. Deininger, N. Shah, F. McCormick, S. Willis, A. Daridon, M. Unger and J. P. Radich, *Leukemia*, 2009, **23**, 396–399.
38 N. R. Beer, B. J. Hindson, E. K. Wheeler, S. B. Hall, K. A. Rose, I. M. Kennedy and B. W. Colston, *Anal. Chem.*, 2007, **79**, 8471–8475.
39 M. M. Kiss, L. Ortoleva-Donnelly, N. R. Beer, J. Warner, C. G. Bailey, B. W. Colston, J. M. Rothberg, D. R. Link and J. H. Leamon, *Anal. Chem.*, 2008, **80**, 8975–8981.
40 J. Pipper, M. Inoue, L. F. Ng, P. Neuzil, Y. Zhang and L. Novak, *Nat. Med.*, 2007, **13**, 1259–1263.
41 Y. Schaerli, R. C. Wootton, T. Robinson, V. Stein, C. Dunsby, M. A. Neil, P. M. French, A. J. Demello, C. Abell and F. Hollfelder, *Anal. Chem.*, 2009, **81**, 302–306.
42 A. B. Theberge, F. Courtois, Y. Schaerli, M. Fischlechner, C. Abell, F. Hollfelder and W. T. S. Huck, *Angew. Chem., Int. Ed.*, 2010, **49**, 5846–5868.
43 M. Curcio and J. Roeraade, *Anal. Chem.*, 2003, **75**, 1–7.
44 K. D. Dorfman, M. Chabert, J. H. Codarbox, G. Rousseau, P. de Cremoux and J. L. Viovy, *Anal. Chem.*, 2005, **77**, 3700–3704.
45 F. Shen, W. Du, J. E. Kreutz, A. Fok and R. F. Ismagilov, *Lab Chip*, 2010, **10**, 2666–2672.
46 F. Wang and M. A. Burns, *Biomed. Microdevices*, 2009, **11**, 1071–1080.
47 N. R. Beer, E. K. Wheeler, L. Lee-Houghton, N. Watkins, S. Nasarabadi, N. Hebert, P. Leung, D. W. Arnold, C. G. Bailey and B. W. Colston, *Anal. Chem.*, 2008, **80**, 1854–1858.
48 L. Mazutis, A. F. Araghi, O. J. Miller, J. C. Baret, L. Frenz, A. Janoshazi, V. Taly, B. J. Miller, J. B. Hutchison, D. Link, A. D. Griffiths and M. Ryckelynck, *Anal. Chem.*, 2009, **81**, 4813–4821.
49 P. Kumaresan, C. J. Yang, S. A. Cronier, R. G. Blazej and R. A. Mathies, *Anal. Chem.*, 2008, **80**, 3522–3529.
50 A. Russo, V. Bazan, V. Agnese, V. Rodolico and N. Gebbia, *Ann. Oncol.*, 2005, **16**(suppl. 4), iv44–iv49.
51 H. L. Wang, J. Lopategui, M. B. Amin and S. D. Patterson, *Adv. Anat. Pathol.*, 2010, **17**, 23–32.
52 J. Soh, N. Okumura, W. W. Lockwood, H. Yamamoto, H. Shigematsu, W. Zhang, R. Chari, D. S. Shames, X. Tang, C. MacAulay, M. Varella-Garcia, T. Vooder, Wistuba, II, S. Lam, R. Brekken, S. Toyooka, J. D. Minna, W. L. Lam and A. F. Gazdar, *PLoS One*, 2009, **4**, e7464.
53 M. Li, W. D. Chen, N. Papadopoulos, S. N. Goodman, N. C. Bjerregaard, S. Laurberg, B. Levin, H. Juhl, N. Arber, H. Moinova, K. Durkee, K. Schmidt, Y. He, F. Diehl, V. E. Velculescu, S. Zhou, L. A. Diaz, Jr, K. W. Kinzler, S. D. Markowitz and B. Vogelstein, *Nat. Biotechnol.*, 2009, **27**, 858–863.
54 A. Lievre, J. B. Bachet, D. Le Corre, V. Boige, B. Landi, J. F. Emile, J. F. Cote, G. Tomasic, C. Penna, M. Ducreux, P. Rougier, F. Penault-Llorca and P. Laurent-Puig, *Cancer Res.*, 2006, **66**, 3992–3995.
55 L. Mazutis, J. C. Baret and A. D. Griffiths, *Lab Chip*, 2009, **9**, 2665–2672.
56 J. Clausell-Tormos, D. Lieber, J. C. Baret, A. El-Harrak, O. J. Miller, L. Frenz, J. Blouwolff, K. J. Humphry, S. Koster, H. Duan, C. Holtze, D. A. Weitz, A. D. Griffiths and C. A. Merten, *Chem. Biol.*, 2008, **15**, 427–437.
57 P. Laurent-Puig, A. Lievre and H. Blons, *Eur. J. Cancer*, 2009, **45**, 398–399.
58 A. Lievre and P. Laurent-Puig, *Nat. Rev. Clin. Oncol.*, 2009, **6**, 306–307.
59 E. Schonbrun, A. R. Abate, P. E. Steinvurzel, D. A. Weitz and K. B. Crozier, *Lab Chip*, 2010, **10**, 852–856.
60 S. A. Leon, B. Shapiro, D. M. Sklaroff and M. J. Yaros, *Cancer Res.*, 1977, **37**, 646–650.
61 S. Jahr, H. Hentze, S. Englisch, D. Hardt, F. O. Fackelmayer, R. D. Hesch and R. Knippers, *Cancer Res.*, 2001, **61**, 1659–1665.
62 T. Lecomte, N. Ceze, E. Dorval and P. Laurent-Puig, *Gastroenterol. Clin. Biol.*, 2010, **34**, 662–681.
63 F. Diehl, M. Li, Y. He, K. W. Kinzler, B. Vogelstein and D. Dressman, *Nat. Methods*, 2006, **3**, 551–559.
64 E. Brouzes, M. Medkova, N. Savenelli, D. Marran, M. Twardowski, J. B. Hutchison, J. M. Rothberg, D. R. Link, N. Perrimon and M. L. Samuels, *Proc. Natl. Acad. Sci. U. S. A.*, 2009, **106**, 14195–14200.
65 R. Tewhey, J. B. Warner, M. Nakano, B. Libby, M. Medkova, P. H. David, S. K. Kotsopoulos, M. L. Samuels, J. B. Hutchison, J. W. Larson, E. J. Topol, M. P. Weiner, O. Harismendy, J. Olson, D. R. Link and K. A. Frazer, *Nat. Biotechnol.*, 2009, **27**, 1025–1031.
66 Q. Zhong, S. Bhattacharya, S. Kotsopoulos, J. Olson, V. Taly, A. D. Griffiths, D. R. Link and J. W. Larson, *Lab Chip*, 2011, DOI: 10.1039/c1lc20126c.
67 D. Santini, S. Galluzzo, L. Gaeta, A. Zoccoli, E. Riva, A. Ruzzo, B. Vincenzi, F. Graziano, F. Loupakis, A. Falcone, A. Onetti Muda and G. Tonini, *J. Clin. Oncol.*, 2011, e206–e207.
68 L. Benhaim, K. Maley, D. Le Corre, H. Blons, V. Taly, F. Bibeau, J.-F. Emile and P. Laurent-Puig, *J. Clin. Oncol.*, 2011, **29**, e208–e209.
69 J. Li and G. M. Makrigiorgos, *Biochem. Soc. Trans.*, 2009, **37**, 427–432.
70 B. G. Zimmermann, S. Grill, W. Holzgreve, X. Y. Zhong, L. G. Jackson and S. Hahn, *Prenatal Diagn.*, 2008, **28**, 1087–1093.
71 J. Gandhi, J. Zhang, Y. Xie, J. Soh, H. Shigematsu, W. Zhang, H. Yamamoto, M. Peyton, L. Girard, W. W. Lockwood, W. L. Lam, M. Varella-Garcia, J. D. Minna and A. F. Gazdar, *PLoS One*, 2009, **4**, e4576.
72 Y. N. Xia and G. M. Whitesides, *Angew. Chem., Int. Ed.*, 1998, **37**, 551–575.
73 C. Holtze, A. C. Rowat, J. J. Agresti, J. B. Hutchison, F. E. Angile, C. H. Schmitz, S. Koster, H. Duan, K. J. Humphry, R. A. Scanga, J. S. Johnson, D. Pisignano and D. A. Weitz, *Lab Chip*, 2008, **8**, 1632–1639.
74 S. L. Anna, N. Bontoux and H. A. Stone, *Appl. Phys. Lett.*, 2003, **82**, 364–366.
75 L. Mazutis, J. C. Baret, P. Treacy, Y. Skhiri, A. F. Araghi, M. Ryckelynck, V. Taly and A. D. Griffiths, *Lab Chip*, 2009, **9**, 2902–2908.

